FIRE2: A NEW APPROACH FOR PREDICTING THERMAL RADIATION LEVELS FROM HYDROCARBON POOL FIRES

M.J. Pritchard and T.M. Binding

British Gas plc, Midlands Research Station, Wharf Lane, Solihull,
West Midlands B91 2JW

A methodology has been developed for predicting incident thermal radiation levels around pool fires, following accidental spillages of flammable liquids into bunded areas. A realistic representation of the flame shape has been developed using new correlations for predicting the flame geometry. The model has been validated against data from a wide range of experiments and good agreement obtained between model predictions, observed flame shapes and measured thermal radiation levels. It can be used to assess the consequences of LNG, ethane, propane, butane, naphtha and kerosene pool fires, in bunds of various dimensions and over a range of weather conditions.

Pool Fire, Thermal Radiation, LNG, Hydrocarbon, Computer Modelling

1. INTRODUCTION

Safe operation and accident prevention have been primary considerations in the development of the oil and gas industry. As a result, present day facilities are designed, constructed and operated to high safety standards.

In addition to the industries' own efforts to ensure the highest standards of safety, regulations for the control of major industrial sites storing or processing dangerous materials have been implemented. These regulations often require that safety assessments are undertaken, in order to quantify the hazards associated with site operations. Information from such assessments is essential for the preparation of appropriate on-site and off-site emergency plans. Within the European Economic Community, the Council Directive on Major Accident Hazards(1) has required member countries to adopt such legislation. In the U.K., this is enacted through the Control of Industrial Major Accident Hazards (CIMAH) Regulations(2).

Detailed safety assessments require methodologies for calculating as accurately as possible the consequences of a range of accidental release scenarios. In particular, the release and ignition of a liquid fuel such as LNG may result in a pool fire which would subject the surroundings and adjacent plant or equipment to thermal radiation and possibly flame impingement.

This paper describes a new model, FIRE2, which has been developed by British Gas to assess the hazards presented by liquid hydrocarbon pool fires contained within bunded areas. The model can be applied to fires involving a range of fuel types, pool shapes and pool sizes and can be used to determine the levels of incident thermal radiation at any position around the fire and onto surfaces at any inclination or orientation. Predictions can be made over a range of weather conditions. The model is based on data obtained from a wide

range of large scale experiments, and has been validated against further experimental data.

2. LARGE SCALE POOL FIRE EXPERIMENTS

Predictions of thermal radiation levels produced as a function of distance from a pool fire are usually obtained from models based on experimental measurements of flame geometry and radiative characteristics. The characteristics of flames associated with large hydrocarbon pool fires have been studied by a number of workers(3-11). Experiments have been conducted in circular, rectangular and square bunds with most of the studies providing information on the characteristics of LNG pool fires, although data are available for other fuels ranging from LPG to crude oil. Detailed reviews of previous work have been undertaken(6-8,12).

Many of the processes involved in the emission of thermal radiation from burning pools of hydrocarbon liquids are scale dependent(8). The shape and size of the flame will depend upon the thermodynamic properties of the liquid involved, and on the pool shape and size. The effects of buoyancy and the wind conditions are also important. Development and validation of models to predict thermal radiation levels is thus dependent on obtaining data on the effects these parameters have on fire characteristics.

Therefore, it is important to obtain data from experiments which are conducted as close as practicable to full scale. Although difficult and expensive to perform, such experiments have been undertaken, for example as depicted in Figure 1a, with LNG contained in low aspect ratio shallow rectangular bunds(6) (up to 15.2m square) and circular bunds(8,22) (up to 35m diameter). These experiments have shown that buoyancy has an increasing effect on flame shape as pool size increases. Increases in pool size also lead to increasing values of the flame surface emissive power, probably associated with increasing soot formation in the fire. Additionally, the mass burning rate was found to increase with pool size, leading to proportionately shorter duration fires. However, data obtained from the 35m diameter LNG pool fire experiments have indicated that for both the flame surface emissive power and the mass burning rate, limiting values may have been approached.

The behaviour of fires burning in tank tops or high walled bunds has been examined in experiments carried out in high walled bunds up to 10.7m in diameter. These experiments have shown that, compared to fires in shallow bunds, fires in high walled bunds can result in an increase in the extent of the flame downwind beyond the edge of the bund.

Experiments with higher hydrocarbons burning in shallow bunds, have shown that the flame surface emissive power increases more rapidly with pool size than for LNG(7,13). However, above a critical value of fire size, radiative heat loss from the flame leads to quenching of the chemical reactions which consume soot. This produces an increasing tendency with increasing pool size to generate black smoke(7,13), screening the thermal radiation from much of the flame, as shown in Figure 1b, and in some cases leading to a significant reduction in the total radiative output from the fire. Although less pronounced, smoke shielding of the upper part of the flame was also observed during large LNG pool fires(8).

Overall, experiments have demonstrated that scale is important in assessing both the radiative and geometric characteristics of fires, and that soot and smoke formation need to be allowed for properly in predicting the thermal radiation hazards from liquid pool fires.

3. FIRE2 MODEL

For any receiver adjacent to a liquid hydrocarbon pool fire, the incident thermal radiation (I) is determined using the following equation:

$$I = F. SEP. \tau \quad (1)$$

where F is a configuration factor, SEP is the surface emissive power of the flame and τ is the atmospheric transmissivity. The configuration factor enables the relative position and geometry of the flame and receiving object to be taken into account. The atmospheric transmissivity is an important parameter in the model, as it takes account of the amount of radiation absorbed by the intervening atmosphere and the receiver. Atmospheric transmissivity is primarily dependent upon the amount of water vapour in the atmosphere and the path length between the flame and the receiver(21).

In order to predict accurately the thermal radiation field around a pool fire, a knowledge is required of three factors; the flame geometry and hence the configuration factor, the thermal radiative characteristics of the flame and the atmospheric transmissivity. How these have been incorporated into the new British Gas pool fire model, FIRE2, is discussed in detail in the following sections.

3.1 Flame Geometry

In previous models, the shapes of flames associated with large hydrocarbon pool fires have been approximated using regular geometrical shapes, either as a cone(6), a sheared cylinder(7,14) or a tilted cylinder(3,4,6). Analytical expressions for calculating the configuration factors have been derived using a geometrical determination technique(15) or the contour integral method(16). Such equations are available for cylinders and other simple shapes, but are restricted to certain locations and orientations of the receiver. A number of area integral methods have also been developed(17,18) to define an approximate flame shape. In these methods the shape representing the flame is split into a series of parallelograms or triangles. Correlations were then developed(6,14,19) for a time averaged flame length and flame tilt. Some workers also produced a correlation for the flame drag(6,14), the extent to which the flame base extends outside the bund in a downwind direction. Care needs to be taken in comparing the correlations developed by the various groups of workers, as the geometrical parameters, in particular the flame length, are often defined in different ways.

Comparison with experimental data has shown that representing a pool fire by a cylindrical or other simple shape can result in inaccurate predictions of thermal radiation levels at positions close to the fire. For large fires in particular, the cylindrical representation results in a shape which extends further downwind than is actually observed experimentally. In an actual fire(8), buoyancy forces result in much of the top half of the flame being

tilted less than the lower part. Thus, for downwind receivers, the models based on a cylindrical flame shape predict higher radiation levels than are observed experimentally, with the difference increasing with fire size.

The FIRE2 model is based on the area integral method described by Hankinson(18), with the flame envelope split into small triangular elements. The use of triangles increases the scope to develop a more complex and therefore more realistic representation of the flame shape and thus overcomes many of the geometrical shortcomings discussed above. This realistic flame shape has been derived from time-averaged flame shapes measured during numerous large scale LNG pool fire experiments, with effective bund diameters ranging from 6.1m to 20.0m(5,6,22). The observed shapes were digitised and normalised to remove the effect of the pool size, flame length and flame tilt (Figure 2). The normalised shapes produced were in excellent agreement with each other, and resulted in the identification of a single normalised shape.

Correlations were developed from LNG pool fires in bunds from 6.1m to 35m diameter(5,6,8,22), and from fires involving fuels other than LNG in bunds up to 20m diameter, to produce general scaling relationships for use in FIRE2 for the flame length, flame tilt, flame drag and the mass burning rate. Figure 3 shows the definitions of the geometrical parameters used in the model.

3.1.1 Maximum Flame Length. Various correlations are available in the literature to predict the length of flames in fires burning above liquid hydrocarbon pools, although care should be used in comparing them as the flame length is not always defined in the same way. Each correlation does however relate the flame length to similar dimensionless groups, in particular the dimensionless mass burning rate. Commonly used correlations for flame length include those published by Thomas(19), the AGA(3) and Moorhouse(6). None of these correlations are suitable for calculating flame lengths for use in a model using a realistic flame shape as they are based on idealised flame shapes. The Thomas equation tends to underestimate the measured maximum time-averaged flame length for the majority of experiments, particularly for larger fires. The AGA equation, however, tends to over-predict the data. The correlation obtained by Moorhouse for a cylindrical flame representation significantly underpredicts the maximum flame length, while that for a conical flame representation is the best of the currently available correlations.

For use within FIRE2, a new correlation has been developed for predicting the maximum flame length, L_m, based on the same dimensionless groups used in previously published models. No dependence on fuel type was observed, and thus fuel-dependent terms were not included in the correlation:

$$L_m = 10.615 \ (m^*)^{0.305} \ (U^*_9)^{-0.03} \ D_H \qquad (2)$$

where m^* and U^* are the dimensionless mass burning rate and windspeeds respectively (the subscript 9 denotes that the windspeed was measured at a height of 9m), and are given by:

$$m^* = m \ / (\rho_a \sqrt{gD_H}) \qquad (3)$$

and

$$U^*_9 = U_9/U_c \ , \text{ and } \ U_c = (gmD_H/\rho_a)^{1/3} \qquad (4)$$

In equation (4), U^*_9 is constrained to be no less than 1. (i.e. $U^*_9 \geq 1$)

The correlation given by equation (2) provides a good fit to the experimental

data and measured values of the maximum flame length are shown plotted against predicted values in Figure 4.

3.1.2 Flame Tilt. Many of the correlations available in the literature relate the flame tilt to either the dimensionless windspeed or Froude number. Thomas's equation(19) consistently underpredicts the experimentally obtained flame tilt angle, while the AGA(3) equation tends to overpredict. Both of the correlations produced are of the form:

$$\cos\Theta = A \ (U^*)^B \qquad (5)$$

where A and B are constants. The main shortcoming of this form of equation is that U^* is taken to be unity, and the flame tilt zero, when the measured windspeed is less than the characteristic windspeed (U_c). This can result in inaccurate predictions for large diameter fires burning in low windspeeds, since a small change in windspeed will result in a large change in the predicted flame tilt, whereas experimental data indicates that flame tilt still occurs with very low windspeeds. This problem was overcome by the equation developed by Welker and Sliepcevich(14) and discussed by Moorhouse(6), which related the tilt to the Froude and Reynolds numbers. The parameters used in their equation have been fitted to the experimental data to produce the following equation which is used in FIRE2:

$$\tan\Theta/\cos\Theta = 0.666 \ (Fr)^{0.333} \ (Re)^{0.117} \qquad (6)$$

Where Fr is the Froude number and Re is the Reynolds number of the source, given by:

$$Fr = U_9^2/gD_H \qquad (7)$$

$$Re = D_H U_9/\gamma \qquad (8)$$

The data does not indicate a relationship between the flame tilt and fuel type and therefore the correlation does not incorporate the term for gas vapour density used by Welker and Sliepcevich(14). The experimentally measured values for the ratio of $\tan\Theta/\cos\Theta$ obtained by the correlation are shown plotted against the values predicted by Equation (6) in Figure 5. To allow for buoyancy effects, this tilt is only applied to the lower half of the flame. Based on the experimental data, the model uses an angle of $\Theta/2$ applied to the upper half of the flame.

3.1.3 Flame Drag. Flame drag, or flame base extension, is a phenomenon which has been observed in all the experiments conducted by British Gas. However, the AGA(3) equations used to describe the flame shape do not include a correlation for this phenomenon, although photographs taken during their LNG pool fire experiments showed that the effect was present. No flame drag effect was reported by Thomas(19) for burning wooden cribs. Welker and Sliepcevich(14) did, however, note this effect, as did Moorhouse(6). However, the correlations obtained by these sets of workers are not in good agreement with the more recent experimental data which is now available.

The experimental data indicated that the flame drag was dependent on fuel type, and therefore there is a need to obtain a correlation for the flame drag that adequately accounts for the fuel type. A ratio term to account for gas vapour density has therefore been included in the equation that has been

produced to describe this effect. The correlation produced is given by:

$$D'/D_H = 2.506\ (Fr)^{0.067}\ (Re)^{-0.03}\ (\rho_g/\rho_a)^{0.145} \quad (9)$$

Where D'/D_H is the flame drag ratio. Measured values of the flame drag ratio are shown plotted against values predicted using the correlation given in Equation (9) in Figure 6. Excellent agreement was obtained for all fuel types.

3.2 Mass Burning Rate

The mass burning rate is an important parameter in any model as it is used in several of the correlations described in Section 3.1, as well as for predicting the overall duration of the fire. Experiments have shown that the mass burning rate has a strong dependence on bund size with a weaker dependence on fuel type(6-8). The dependence on pool size is primarily due to the variation of the flame surface emissive power (SEP) with pool size (see Section 3.3). SEP increases with pool size up to a limiting value, which occurs at different pool sizes for each fuel. Thus, the back radiation to the liquid surface will be higher for larger pool diameters, producing an increase in the vapour evolution rate. Eventually, a limiting value of the mass burning rate will be reached (as a result of the limiting SEP - see Section 3.3.1). An exponential relationship to the data was therefore derived to incorporate the limiting value of mass burning rate. For LNG and ethane the mass burning rate within FIRE2 is given by:

$$m = 0.14\ (\ 1 - \exp(-0.156D_H)) \quad (10)$$

For LPG pool fires the relationship used in FIRE2 is given by:

$$m = 0.12\ (\ 1 - \exp(-0.5D_H)) \quad (11)$$

Due to limited experimental data, FIRE2 uses a single value of mass burning rate for other fuel types. The recommended maximum mass burning rate values for a variety of fuels are given in Table 1.

3.3 Thermal Radiative Characteristics of the Flame

Experiments(5,6,8) have shown that in LNG pool fires, a relatively clean flame is produced with some smoke emanating mainly from the top. However, higher hydrocarbon pool fires produce a larger quantity of smoke which obscures part of the flame(5,7), and are characterised by a lower region which is mainly clear flame and an upper region consisting of smoke obscured flame. Most pool fire models assume that the fires emit thermal radiation uniformly over their surface, even though they may consist of regions of flame and smoke.

The radiative properties of a flame are usually represented by an average surface emissive power (SEP), which is calculated from the flame area and measurements of incident thermal radiation. It is therefore dependent upon the flame geometry used to interpret the data. It is important when comparing data on SEPs that the method of calculation is known.

Two different approaches can be used to obtain the SEP. In the first(7) the SEP is based on the actual area of visible flame, whereas in the second the

radiant emission is averaged over an idealised representation of the flame shape(3,5) which may include portions of the flame shielded by smoke. For a fire with any degree of smoke shielding, the latter method produces lower values of SEP, and an under-prediction of the radiation levels in the near field. In the 35m diameter Montoir LNG pool fires discussed by Nedelka et al(8), the SEP based on the clear flame was 50 per cent higher than that calculated using a simple cylindrical shape to represent the flame. Thus, for receivers within a few bund diameters of a pool fire, models using an SEP based on the simple shape are likely to underpredict the received radiation. Several workers(7,20) have split the flame into two zones, a lower one with a high SEP and an upper one with a lower SEP. These two zone models have not previously been applied to LNG, although the Montoir 35m pool fires suggest a two zone approach is appropriate.

In the FIRE2 model, the value of SEP which is adopted is based on experimental values obtained using only the clear flame. For pool fires other than LNG and ethane in small diameter bunds, this approach leads to the adoption of a two zone approach to characterising the thermal radiative output from a flame. This approach has been used previously(8,13), with the flame split into two zones, the lower part having a higher SEP than the upper part, to allow for the smoke shielding. Therefore, to allow for fires where smoke shielding occurs, two additional parameters are included, a clear flame length and an unobscured ratio which defines the proportion of the visible flame area within the upper, partially smoke shielded portion of the flame (Figure 3).

The flame surface emissive power, clear flame length and unobscured ratio are discussed in more detail in the following sections.

3.3.1 Flame Surface Emissive Power. The flame surface emissive power defines the radiant heat emission from a flame and in the case of black body emitters is related to the flame temperature by the Stefan Boltzman equation. The data for SEP obtained from LNG pool fire experiments suggest that although SEP initially increases with pool diameter, there is a limiting value at larger diameters. This limit appears to have been approached during the 35m diameter pool fires(8), and as a result, an exponential fit was used in developing the correlation for SEP which is used in FIRE2. The correlation for average SEP is based on the assumption that thermal radiation is only emitted from the visible parts of the flame (i.e. not obscured by smoke), and is given by:

$$SEP = 265\ (\ 1 - \exp(-0.149D_H)) \quad (12)$$

For fuels other than LNG, a single surface emissive power value is used within FIRE2. To obtain a representative value for each fuel type, an average value of emissive power was obtained from the experiments carried out by British Gas. The recommended values are listed in Table 1. As for LNG the values are based on the assumption that radiation is only emitted from the visible flame.

3.3.2 Clear Flame Length. The clear flame length is defined as the distance along the flame axis from the base of the flame to the upper limit of the flame region which is unobscured by smoke (Figure 3). The experimental data(7) suggest that the clear flame length is dependent on fuel type and pool size, with the length being shorter for higher hydrocarbons and, for a given fuel, for increasing pool diameters.

Therefore, when producing a suitable correlation for the clear flame length, it was important to include a term to allow for the effects of fuel type and bund diameter. To achieve this, a fit of the same form as for the maximum flame length was attempted, but incorporating a parameter to account for different fuel types. The gas density, ρ_g, was substituted for the air density, ρ_a, in Equation (4), but the fit obtained did not fully account for the difference between fuel types. It was then attempted to obtain correlations using other fuel dependent parameters, i.e. an air density to gas density ratio, and also a carbon to hydrogen ratio. The latter method was adopted because it is more important in determining the degree of smoke formation in the flame and gives a good fit for heavy hydrocarbons as well as for LNG. The correlation is given by:

$$L_c = 11.404 \quad (m^*)^{1.13} \quad (U^*_g)^{0.179} \quad (C/H)^{-2.49} \quad D_H \qquad (13)$$

Measured values of the clear flame length are shown plotted against predicted values obtained from Equation (13) in Figure 7.

3.3.3 Unobscured Ratio. The unobscured ratio of the flame is the parameter used to take account of the amount of smoke obscuration of the upper region of the flame. It is defined as the ratio of the total area of visible flame in the upper region to the total area of the upper region. The unobscured ratio will be dependent upon the flame shape adopted; in FIRE2, the normalised shape described in Section 3.1 is used. For fires which produce little smoke, for example most LNG fires, the unobscured ratio will be high, whereas low values will be obtained for fires involving significant soot production, for example, kerosene fires.

Values of unobscured ratio were obtained from measurements obtained from many of the experiments which have been conducted. The data show that there is a strong dependence on pool diameter and fuel type. From the measured data different values for the unobscured ratio were selected for varying fuel type and pool diameter. The data were divided into three categories based on pool size; less than 10m diameter, 10 to 20 m diameter, and 20m diameter and above. The values obtained are given in Table 2, and are intended to represent average values for each fuel type and pool size category.

As the model calculates an SEP based on the extent of the visible flame, for the upper portion of the flame, where there is significant smoke obscuration, this is multiplied by the unobscured ratio to give a lower, 'effective' SEP.

3.4 Configuration Factor

Once a flame shape has been produced by the model, a configuration factor can be obtained. The FIRE2 model uses an area integral method(18) to calculate the configuration factor. The flame shape is split into 50 horizontal bands, each of which is split into 336 small triangular elements. Conditions are then applied to select only those elements on the flame surface which can be seen by a receiver at a given position and orientation. A configuration factor is obtained between each of these triangles and the receiver, with the sum from all viewed triangles representing the overall configuration factor.

4. FIRE2 VALIDATION AND CAPABILITIES

To be an effective model, it is important that FIRE2 provides accurate predictions of incident thermal radiation levels generated by liquid pool fires at receiver positions for a wide range of pool geometries, fuel types and weather conditions, both upwind, crosswind and downwind of the fire. In reality, the predictions of the model for locations downwind of the fire are likely to be used for safety assessments, so it is particularly important to predict accurately the incident thermal radiation in that direction.

The ambient windspeed and pool diameter must be specified in order to produce a representative flame shape for a particular scenario from the general normalised flame shape. These parameters, applied to the correlations discussed in Section 3, enable FIRE2 to produce a flame shape that is a much better representation of the observed flame shape than that given by a simple shape, such as a cylinder (Figure 8). In zero wind conditions the representative flame shape has a circular cross-section and in wind blown conditions an ellipsoidal one.

Validation of the model has been achieved by comparing predictions from FIRE2 with a wide variety of data that have been obtained from experiments. This is achieved by calculating the incident thermal radiation levels at locations corresponding to positions where radiation levels were measured during the experiments. In this way, measured values can be directly compared with predicted values of incident thermal radiation levels. The model has been validated against data obtained from a large number of pool fires, with varying fuel types and geometries, including experiments conducted by both British Gas and other workers.

Figure 9 shows measured incident thermal radiation (flux) values obtained from experiments conducted with fuels other than LNG in low-walled rectangular bunds, plotted against values predicted by FIRE2. The data obtained from Welker and Cavin(11) were for nominally 20ft square propane pit fires. The British Gas data were obtained from fires burning in rectangular bunds with hydraulic diameters of approximately 7 and 14m. It is apparent from this figure that the model provides good predictions of the data obtained from experiments and can therefore be used with confidence for fuels other than LNG.

The model has also been validated against a wide range of circular, LNG fires in shallow bunds. Excellent agreement was obtained between the FIRE2 predictions and data obtained from the 35m LNG pool fire reported by Nedelka et al(8), as shown in Figure 10, even though these experiments were not used in deriving the flame shape used in the model.

The FIRE2 model can be used for pool fires involving LNG, ethane, propane, butane, naphtha and kerosene, and can be applied to enable the user to predict incident thermal radiation levels at any given position. Alternatively, the model can be used to predict the distance to a given thermal radiation level. When applying the model to consider the effect of a pool fire on adjacent plant, it is important to be able to predict the total heat loading received, in order to assess if fire protection is required. The FIRE2 model can provide this information by computing values of incident radiation at different locations over the receiving surface, which can then be integrated to obtain the total heat load.

For some applications it may be necessary to determine the orientation of a receiver at a particular location which would be subjected to the maximum level of thermal radiation. A technique to calculate the maximum radiation levels and the corresponding orientation is included in the model. The model can be applied to fires burning in both shallow and high walled circular bunds and also to shallow rectangular bunds with aspect ratios of less than 2.5:1.

5. CONCLUSIONS

A new model, FIRE2, has been developed by British Gas which accurately predicts thermal radiation levels from liquid hydrocarbon pool fires burning in bunded areas. A realistic representation of observed flame shape has been derived and used with new correlations for flame geometry parameters, to give good agreement between thermal radiation levels measured in experiments and those predicted by the model. The model allows the extent of any pool fire hazard to be assessed more accurately than existing approaches and hence, for example, enables the need for fire protection or fire prevention systems to be determined.

6. NOMENCLATURE

m^*	dimensionless mass burning rate
U^*	dimensionless windspeed
L	maximum flame length (m)
D^m	hydraulic bund diameter (m)
m^H	mass burning rate ($kgm^{-2}s^{-1}$)
ρ_a	air density (kgm^{-2})
U^a	windspeed (ms^{-1})
U	characteristic windspeed (ms^{-1})
ρ^c	gas density (kgm^{-2})
g^g	acceleration due to gravity (ms^{-2})
L	clear flame length (m)
(C/H)	carbon to hydrogen ratio of fuel
Θ	flame tilt angle
Fr	Froude number
Re	Reynolds number
γ	kinematic viscosity (m^2s^{-1})
D'/D	flame drag ratio
SEP^H	surface emissive power (kWm^{-2})
F	configuration factor
I	incident thermal radiation (kWm^{-2})
τ	atmospheric transmissivity

7. ACKNOWLEDGEMENTS

The authors would like to thank their many colleagues whose work has provided an input to the various aspects of this paper. The paper is published by permission of British Gas plc.

8. REFERENCES

1. 1982. European Council Directive on the Major Accident Hazards of Certain Industrial Activities, 82/501/EEC.

2. 1984. Control of Industrial Major Accident Hazards Regulations, HMSO, London, S.I. 1984/1902.

3. AMERICAN GAS ASSOCIATION, 1973. Project 1S-3-1.

4. RAJ, P.K., MOUSSA, A.N. and AVRAMUDAN, K., 1979. Report No.CG-D-55-79, U.S. Dept. of Transport.

5. MIZNER, G.A. and EYRE, J.A., 1982. I.Chem.E. Symposium Series No.71, pp 147-163.

6. MOORHOUSE, J., 1982. I.Chem.E. Symposium Series No.71, pp165-179

7. MOORHOUSE, J. and PRITCHARD, M.J., 1988. European Seminar on the Pressurised Storage of Flammable Liquids, IBC Tech. Services, London.

8. NEDELKA, D., MOORHOUSE, J. and TUCKER, R.F., 1989. 9th International Conference on Liquefied Natural Gas, Nice, Session 3, Paper 3.

9. MAEZAWA, M., 1973. Japan Society for Safety Engineering.

10. HAGGLUND,B. and PERSSON,L., 1976. Forsvarets Forskningsanstalt, Stockholm, FOA Report C 20126-D$ (A3).

11. WELKER,J.R. and CAVIN,W.D., 1981. U.S. Dept. of Energy, DOE/EP-0042.

12. LOWESMITH, B.J, MOORHOUSE, J.M., PRITCHARD, M.J., and ROBERTS, P., 1992. 10th International Conference on Liquefied Natural Gas, Kuala Lumpur.

13. WAYNE,F.D., and KINSELLA,K., 1984. ASME Winter Meeting 84-WA/HT=74, New Orleans.

14. WELKER, J.R. and SLIEPCEVICH, C.M., 1966. Fire Technology, Vol. 2, pp127-135.

15. MCGUIRE, J.H., 1953. Fire Research Special Report No.2, HMSO, London.

16. SPARROW, E.M. and CESS, R.D., 1966. Radiation Heat Transfer, Brooks/Cole Publishing Company.

17. REIN, R.G., SLIEPCEVICH, C.M. and WELKER, J.R., 1970. J. Fire and Flammability, Vol.1.

18. HANKINSON, G., 1983. Fire Safety Science - Proceedings of the First International Symposium.

19. THOMAS, P.H., 1963. 9th Symposium (Int) on Combustion, pp844-859.

20. CONSIDINE, M., 1984. Safety and Reliability Directorate, UKAEA, SRD R297.

21. KONDRATYEV, K.Y., 1965. Radiative Heat Exchange in the Atmosphere., Pergaman Press, New York.

22. British Gas and Shell 6.1m and 10.6m diameter LNG pool fires, unpublished work.

TABLE 1. LIMITING MASS BURNING RATES AND EMISSIVE POWERS

Fuel Type	Mass Burning Rate ($kgm^{-2}s^{-1}$)	Surface Emissive Power (kWm^{-2})
LNG	0.14	265
Ethane	0.14	250
Propane	0.12	250
Butane	0.12	225
Kerosene	0.10	200
Naphtha	0.10	200

TABLE 2. UNOBSCURED RATIOS FOR VARIOUS POOL DIAMETERS

Fuel Type	$D_H < 10m$	$10m \leq D_H < 20m$	$D_H \geq 20m$
LNG	1.0	0.9	0.7
Ethane	1.0	0.9	0.7
Propane	0.55	0.3	0.2
Butane	0.3	0.15	0.1
Kerosene	0.02	0.02	0.02
Naphtha	0.3	0.15	0.1

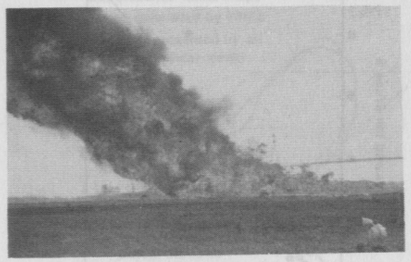

FIGURE 1a. LNG POOL FIRE

FIGURE 1b. LPG POOL FIRE

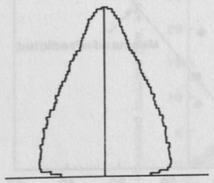

FIGURE 2. TYPICAL NORMALISED FLAME PROFILE

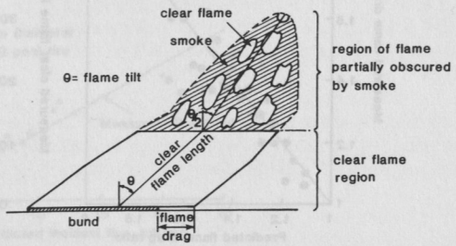

FIGURE 3. TWO-ZONE FLAME REPRESENTATION USED IN THE BRITISH GAS FIRE2 MODEL

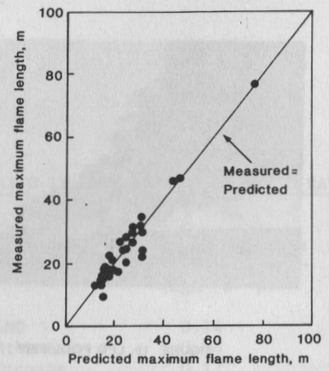

FIGURE 4. A COMPARISON OF MEASURED MAXIMUM FLAME LENGTHS WITH THOSE PREDICTED BY FIRE2

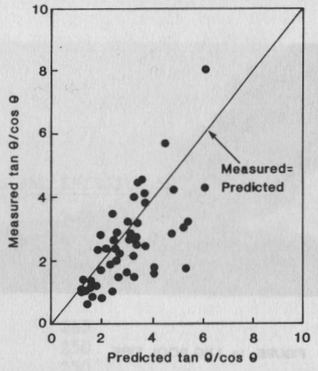

FIGURE 5. A COMPARISON OF MEASURED FLAME TILT ANGLES WITH THOSE PREDICTED BY FIRE2

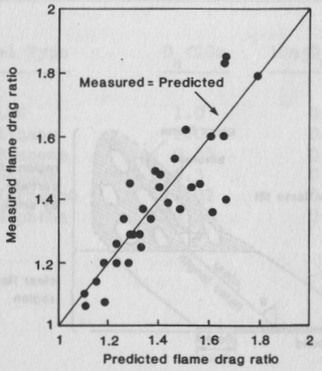

FIGURE 6. A COMPARISON OF MEASURED FLAME DRAG RATIOS WITH THOSE PREDICTED BY FIRE2

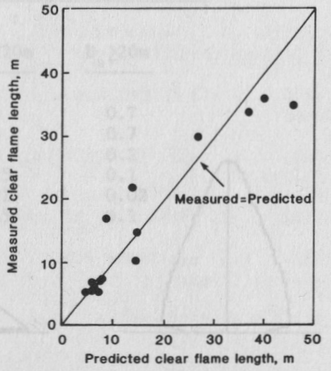

FIGURE 7. A COMPARISON OF MEASURED CLEAR FLAME LENGTHS WITH THOSE PREDICTED BY FIRE2

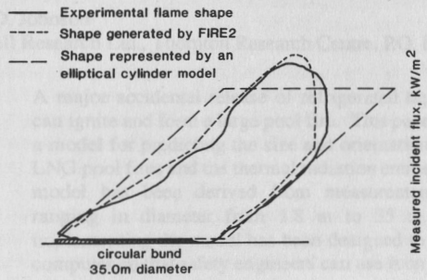

FIGURE 8. COMPARISON OF PREDICTED FLAME SHAPE WITH EXPERIMENT

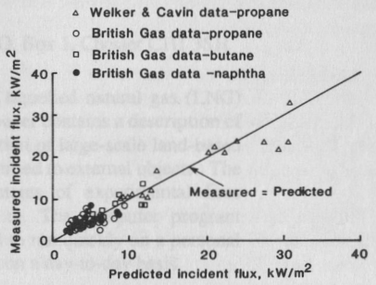

FIGURE 9. A COMPARISON OF MEASURED INCIDENT FLUX VALUES WITH THOSE PREDICTED BY FIRE2

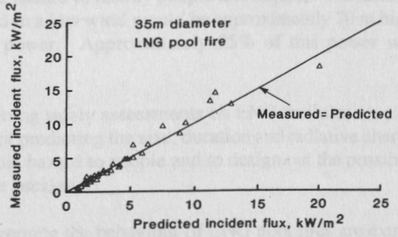

FIGURE 10. A COMPARISON OF MEASURED INCIDENT FLUX VALUES WITH THOSE PREDICTED BY FIRE2